Sensors and Materials, Vol. 35, No. 8 (2023) 3031–3044
MYU Tokyo

S & M 3372

Prediction of Three-phase Four-wire Circuit Balance State Based on Current Sensor Data Fusion and Improved Back Propagation Neural Network

Yiming Zhang,[1] Xiaohua Yang,[1] Tingjie Ba,[2] Yuang Lin,[3*] and Yonghui Zhao[1]

[1]Metrology Center, Yunnan Power Grid Co., Ltd., Kunming 650500, China
[2]Marketing Department, Yunnan Power Grid Co., Ltd., Kunming 650500, China
[3]Faculty of Information Engineering and Automation, Kunming University of Science and Technology, Kunming 650500, China

(Received May 16, 2023; accepted July 26, 2023)

Keywords: three-phase four-wire transformer, balance state prediction, balance control compensation, GA-BP neural network, current sensor

Three-phase unbalance refers to the inconsistency of three-phase current or voltage amplitude in a power system, which is a leading cause of power quality degradation, increased line loss rates, and transformer failures in distribution network systems. In this study, we propose a set of early warning methods for detecting three-phase unbalance states using data fusion from current sensors, current balance rate state analysis, and timing prediction. The proposed method utilizes the data collected from current sensors in a smart metering system to establish timing data for current unbalance rates through the calculation of unbalance degree and the coding of unbalance states. The parameters of a backpropagation (BP) neural network are optimized using a genetic algorithm (GA) to improve prediction accuracy by determining optimal values for neuron weights and thresholds during network training. Finally, a current balance state timing prediction model based on the GA-BP algorithm is established and validated using the collected data to verify its accuracy and feasibility. While the overall early warning system may require more precise current sensors to provide stable and accurate electrical energy data for prediction, the proposed method can achieve a balanced situational awareness of the three-phase power system and provide an effective decision-making basis for deep security defense, and take the necessary measures in a timely manner to respond to the problems encountered in the power system.

1. Introduction

With the rapid economic development in various regions, the demand for electrical energy has significantly increased, especially in low-voltage residential areas where a three-phase four-wire distribution network system is commonly used.(1) Power transformers play a critical role in the power transmission system, and their failure can result in direct and indirect losses to power users, as well as negatively impact the overall stability of the power system.(2,3) In a three-phase

*Corresponding author: e-mail: 18087147030@163.com
https://doi.org/10.18494/SAM4520

ISSN 0914-4935
https://myukk.org/

four-wire distribution system, maintaining a balanced state can be challenging,[4,5] as it involves various factors such as unbalanced transformer capacity, different winding distributions, improper coil connection, and leakage between transformer windings. Severe unbalance in the line system can lead to a significant decline in power quality, increased line losses, reduced power conversion efficiency, and even transformer failure.[6]

Currently, there has been significant research focus on the balance control of three-phase four-wire circuits. Zheng conducted a study on mechanical equipment fault prediction using multidimensional timing data, such as current.[7] Cui *et al.* proposed a timing prediction method based on discrete Fourier decomposition for power imbalance prediction,[8] while Weng *et al.* studied power quality prediction on the basis of clustered long short-term memory neural network deep learning.[9] However, most studies[10–13] have focused on analyzing technical methods for current balance compensation in three-phase four-wire transformers, and while these compensation technologies have become more mature, they often suffer from the limitations of aging control equipment, resulting in temporary and less effective power balance. Moreover, there is still a lack of research on prediction methods for power-quality-related indicators and the timely detection of transformer line problems for targeted measures.

Therefore, in this study, we first propose a neural-network-based transformer current balance timing prediction model. Furthermore, we optimize the parameters of the neural network using a genetic algorithm (GA) to improve the prediction accuracy of the model. Finally, we validate the prediction performance of the proposed model using the actual data collected from current sensors in a smart meter metering system with multiple transformer current timing datasets. Through error analysis and comparison with a pure backpropagation (BP) neural network model, we demonstrate the improved prediction accuracy of our proposed model.

2. Current Balance Prediction Model Based on the Genetic Algorithm and BP Neural Network Algorithm

2.1 Introduction of three-phase four-wire transformer

The time series data of current imbalance rate is further obtained on the basis of the current data recorded by a smart meter metering system for a typical station of a three-phase four-wire transformer in a regional power grid collected and collated by the system, which can be regarded as an input–output system determined by a nonlinear relationship, and the time series prediction, which is specifically a process of fitting nonlinear parameters. The schematic diagram of the line system of a three-phase four-wire transformer is shown in Fig. 1.

2.2 Introduction to BP neural network

The BP neural network is a powerful tool for effectively classifying or predicting various parameter-free nonlinear data sets.[14] It is a multilayer feed-forward neural network that processes input signals layer by layer in a forward propagation process. When the output values of the output layer are not within the specified range, the network is adjusted through backward

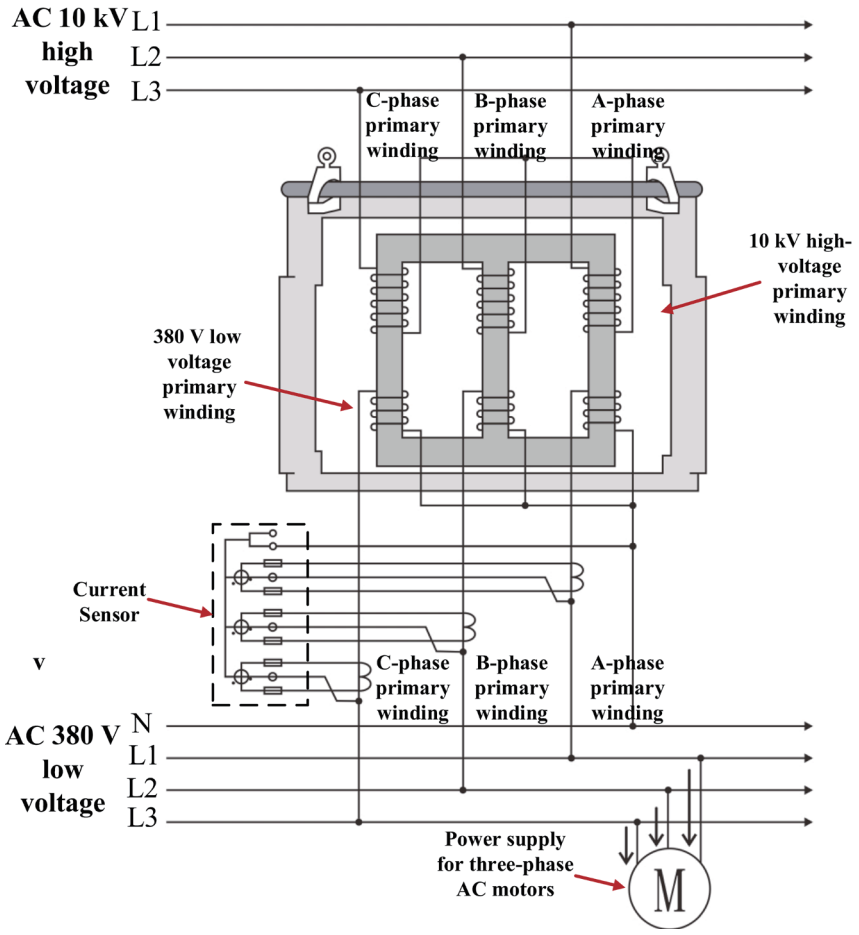

Fig. 1. (Color online) Three-phase four-wire transformer line schematic.

propagation, optimizing the weights of neurons on the basis of the prediction error and threshold to minimize the output error. The topology of the BP neural network is illustrated in Fig. 2, and the main data and parameters involved include input values, output values, neural network weights, and thresholds, as well as the numbers of input and output nodes.

2.3 BP neural network time series forecasting model

During the network training process for current balance timing data, where the input values consist of multiple feature variables and the output values consist of a single variable representing the predicted current balance rate at the next time point, the forward propagation in the output layer can be expressed as

$$\alpha_{kj} = F_j\left(\sum_i w_{ji}\alpha_{ki} + v_j\right), \tag{1}$$

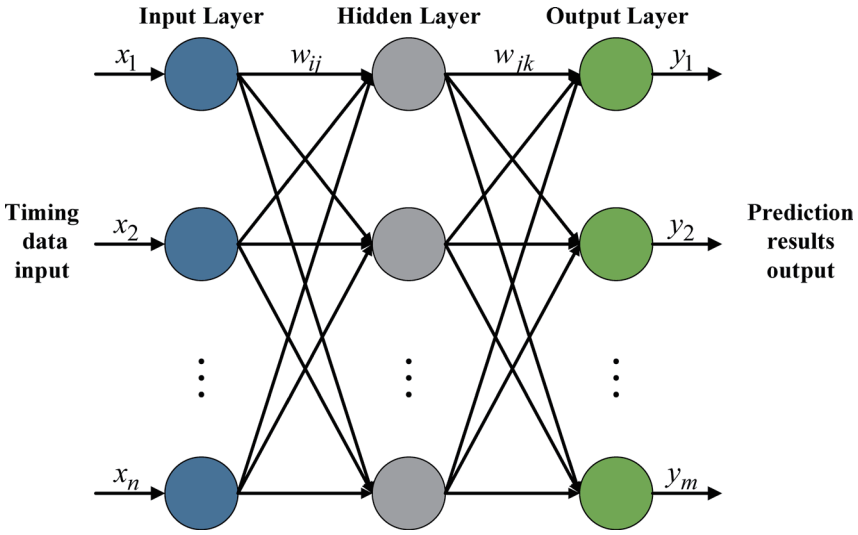

Fig. 2. (Color online) BP neural network topology diagram.

where F_j is the j-th sigmoid-type activation function, w_{ji} represents the weight of the i-th neuron in the previous layer on neuron j in the current layer, α_{kj}/α_{ki} is the information output of sample k in neuron i in the previous layer or neuron j in the current layer, and v_j is the threshold of neuron j in the current layer.

In the forward propagation process, if the output result cannot meet the accuracy, the network will perform layer-by-layer backward transmission error rate. Starting from the output layer, the training error can be expressed as

$$\varepsilon_{kj} = \alpha_{kj}(1-\alpha_{kj})(\lambda_{kj} - \alpha_{kj}). \tag{2}$$

Upon entering the hidden layer, the training error is updated as

$$\varepsilon_{kj} = \alpha_{kj}(1-\alpha_{kj})\sum_{g} \varepsilon_{kg} w_{gj}. \tag{3}$$

The weights are then corrected on the basis of the training error using

$$w_{ji}(\lambda+1) = w_{ji}(\lambda) + \sigma\varepsilon_{kj}\alpha_{kj} + \phi[w_{ji}(\lambda) - w_{ji}(\lambda-1)]. \tag{4}$$

Similarly, the threshold is updated using

$$v_j(\lambda+1) = v_i(\lambda) + \sigma\varepsilon_j + \phi[v_j(\lambda) - v_j(\lambda-1)], \tag{5}$$

where ϕ is a potential factor that helps to reduce the oscillations during network training by affecting the change in past weight with respect to the threshold and σ is the learning rate, which

represents the step size of the gradient search. The learning rate can be set higher when the network does not oscillate during training in order to expedite the training process.

On the basis of the aforementioned network training model, the neural network architecture is employed to learn the diverse sequence patterns inherent in the time series data of current balance rates through nonlinear fitting. This is achieved by utilizing reliable training samples of time series data and effectively storing the information in the network to enhance its pattern discrimination capability. In other words, the network leverages its memory of sequence development patterns to predict the future behavior of the time series.

2.4 Neural network optimization based on GA improvement

Considering the high dependence of the BP neural network on gradient information from training data, in this study, we aim to minimize the global error and achieve the global optimal solution of weights and thresholds in the network by using a GA to improve the BP neural network model.[15] The GA is employed for population-based search to determine the optimal neuron weights and thresholds during the network training process.

To implement this approach, the weights and thresholds are encoded as a set of ordered chromosomes, where each chromosome represents a candidate solution for the network's weights and thresholds. The number of training objects in the chromosomes is represented by real variables in the corresponding dimension, which are part of the encoding operation.

$$A = \left[w_{11}, w_{12}, \cdots w_{mn}, v_1, v_2, \cdots v_m, \lambda_1, \lambda_2, \cdots \lambda_m \right] \tag{6}$$

During the evolutionary process of the GA, the chromosomes are evaluated using a fitness function, which plays a crucial role as the basis for the selection operation. In this study, the fitness function is calculated on the basis of the weights and thresholds of individual neurons in the BP neural network.

$$E(A_i) = \frac{1}{2t} \sum_{k=1}^{t} \sum_{j=1}^{r} (\beta_{kj}^i - \alpha_{kj}^i)^2 \tag{7}$$

$$F(A_i) = E^{-1}(A_i) \tag{8}$$

In the above equation, the variable β_{kj}^i represents the desired output value and α_{kj}^i denotes the output value of the i-th chromosome object, which is determined by the weights and thresholds, for the k-th training object located at node j. The total number of training objects is denoted by t, while r represents the number of neurons in the output layer of the BP neural network. The genetic population size is denoted by N_r. On the basis of these variables, the fitness or adaptation degree $F(A_i)$ of the i-th chromosome can be calculated.

The evolutionary process of the GA includes the following.

2.4.1 Gene selection

On the basis of the adaptation value of an object in the population, the probability of the parent object being included in the offspring is determined using the roulette wheel selection method, which involves proportional selection based on the adaptation value in descending order. Specifically, the higher the adaptation value of an object, the greater its probability of being selected, and vice versa. Mathematically, the probability P_s of an object being selected can be expressed as

$$P_s = \frac{F(A_i)}{\sum_{i=1}^{N_r} F(A_i)}. \tag{9}$$

2.4.2 Gene crossover

On the basis of the crossover operator, the coding structure of the good object is selected from the global optimal perspective. In the following equation, the crossover operation is performed on gene strands A_i and A_j, which have chromosomes a_i and a_j corresponding to a position on the gene strand, and two intermediate variables are set as

$$\Delta_i^1 = \begin{Bmatrix} \min\left\{a_i + \frac{1+P_c}{2}(a_i - a_j), a^{\max}\right\}, & a_i \geq a_j \\ \max\left\{a_i + \frac{1+P_c}{2}(a_i - a_j), a^{\min}\right\}, & a_i < a_j \end{Bmatrix}, \tag{10}$$

$$\Delta_j^1 = \begin{Bmatrix} \min\left\{a_j + \frac{1+P_c}{2}(a_j - a_i), a^{\max}\right\}, & a_i \geq a_j \\ \max\left\{a_j + \frac{1+P_c}{2}(a_j - a_i), a^{\min}\right\}, & a_i < a_j \end{Bmatrix}, \tag{11}$$

where $a^{\max}$ and $a^{\min}$ are the upper and lower bounds of the a_i and a_j values, respectively. The crossover probability P_c is calculated as

$$P_c = \begin{cases} k_1 \dfrac{F_{\max} - F_b}{F_{\max} - F_{avg}}, & F_b \geq F_{avg}, \\ k_2, & F_b < F_{avg}. \end{cases} \tag{12}$$

Here, k_1 and k_2 are constants in the range [0, 1]; $F_{\max}$, F_{avg}, and F_b denote the population maximum fitness, the population average fitness, and the strand with the higher fitness among the crossover pairs, respectively. On the basis of the crossover probability P_c and the random

number φ in the range of [0, 1], some chromosomes of the selected strand are crossed over to obtain two new offspring individuals:

$$s_i = \frac{1+P_c}{2}\Delta_i^1 + \frac{1-P_c}{2}\Delta_j^1, \tag{13}$$

$$s_j = \varphi a_i + (1-\varphi)a_j. \tag{14}$$

This crossover operation enables the child object to perform a new domain search in the region where the parent object is located toward the individual parent object with high adaptation, which improves the efficiency of training and ensures the expansiveness of the genetic population search space.

2.4.3 Genetic variation

The mutation behavior of genes in the GA involves replacing the original gene values with uniformly distributed random numbers, allowing the search process to explore the search space freely and generate new variants of the parent object. The new gene values are calculated using the following formula:

$$\tilde{A}_k = A_{\min} + \rho \cdot \left(A_{\max} - A_{\min} \right), \tag{15}$$

where $A_{\max}$ and $A_{\min}$ represent the maximum and minimum values of the target variables of the initial object, respectively. ρ is a random number uniformly distributed in the range $[0,1]$. This mutation behavior continuously optimizes the coding structure by searching for cues in the space, enhancing the capability to find local optimal solutions and maintaining the diversity of the genetic population.

2.5 GA-BP neural network prediction

In conclusion, the current balance prediction model proposed in this study consists of three main components: BP neural network structure determination, GA optimization, and BP neural network prediction. The flow of the genetic-algorithm-optimized BP neural network algorithm is illustrated in Fig. 3.

When solving the actual GA-BP model, the key step is to determine the appropriate neural network structure, including the number of nodes in the input layer, n, the number of nodes in the output layer, m, and the number of nodes in the hidden layer, S, where the number of hidden layers is generally determined using the empirical formula: $S = \sqrt{n+m} + a, (a = 1, 2, \cdots, 10)$, $S = 2m + 1$, or $S = \sqrt{nm}$. To achieve the best prediction performance, parameters are selected by repeatedly evaluating the training error for different parameter combinations using different prediction datasets.

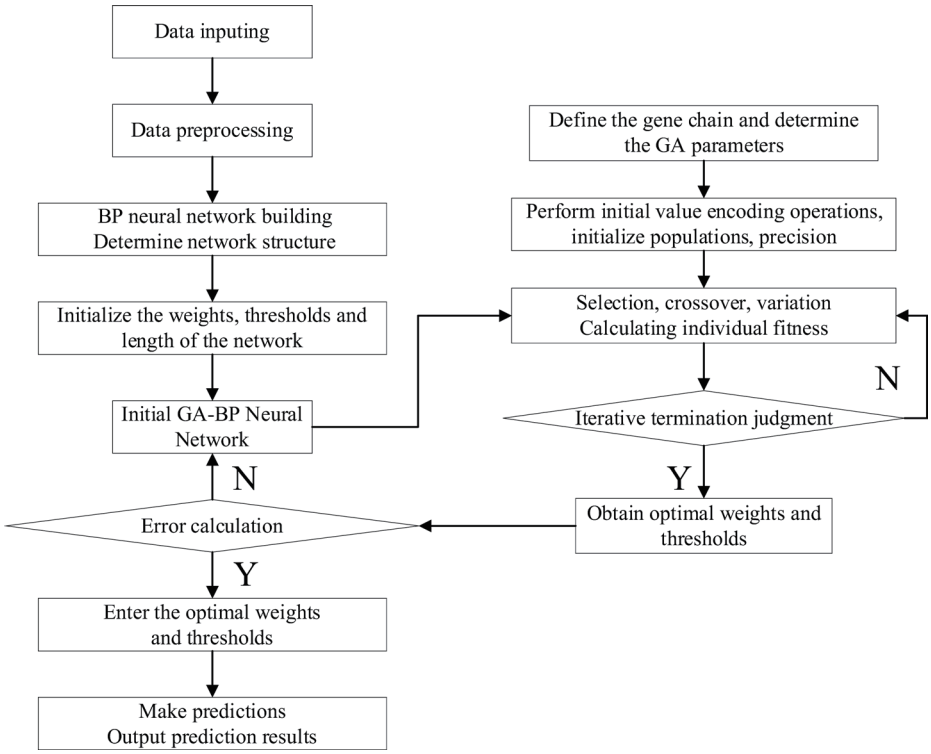

Fig. 3. Improved GA-BP algorithm flow chart.

The optimization process using the GA involves constructing a gene chain based on weights and thresholds and setting the population size, crossover probability, and other GA parameters. During the iteration, the optimal fitness individuals are decoded to provide the optimal weights and thresholds for network training.

3. Current Balance Timing Prediction Based on GA-BP Model

3.1 Timing data preprocessing

The three-phase current unbalance is generally measured using two calculation formulas,[16] namely,

$$\mu_I = \frac{I_{\max} - I_{\min}}{I_{\max}}, \tag{16}$$

and

$$\mu_I = \frac{\max\left\{I_{A/B/C} - I_{avg}\right\}}{I_{avg}}. \tag{17}$$

Here, I_A, I_B, and I_C represent the A, B, and C phase currents, and I_{max} and I_{min} represent the current three-phase maximum and current three-phase average, respectively. The first current unbalance rate calculation method, which is more commonly used locally, is chosen in this study.

To provide a more intuitive representation of the current imbalance degree and evaluate the accuracy of the time series prediction results, a current imbalance code was utilized in this study. The degree of current imbalance was graded on the basis of specific ranges, as presented in Table 1.

In this study, current data from transformers in three representative low-voltage residential customer stations within a regional power grid were collected and compiled over a period of 50 days. The data were recorded in meters at 15 min intervals, and the current imbalance rate was calculated in advance, with the current imbalance degree code assigned according to local rules. However, owing to equipment limitations, there were some missing values in the collected current data. Nevertheless, the impact of these missing values on the prediction results was found to be insignificant after thorough testing and analysis.

3.2 Main parameter setting of GA-BP algorithm

In this study, the established dataset is normalized and used as training samples for the neural network, with every 15 data collection points used for training and the prediction target being the current imbalance rate of the next data collection point. The neural network structure is set with 15 input nodes and one output node, and the time window is continuously shifted to complete the prediction of the entire time series. On the basis of the empirical formula of about five hidden layers, the number of hidden layers is experimented several times, and it was found that the best result is obtained with eight hidden layers.

The specific functions of each parameter of the GA were obtained from the literature.[17] Similarly, several experiments were conducted to select the optimal values for the parameters of the GA, such as the number of genetic generations and the population size.

The population size is typically set between 10 and 200, with larger population sizes resulting in longer computation times and less notable improvement in optimization. Through experimental verification, a population size of 50 is found to yield the best results. The crossover and mutation probabilities are set at 0.8 and 0.1, respectively. The number of generations for genetic evolution is set at 50.

Table 1
Current imbalance code table.

Qualification code of current balance	Range of current balance rate	Significance
1	0–25	Balance
2	25–50	General imbalance
3	50	Severe imbalance

3.3 Analysis of model prediction results

On the basis of the set GA-BP parameters, three sets of preprocessed transformer current balance timing data sets are input into the program and divided into training and test sets in the ratio of 8:2 to perform timing prediction, and the obtained prediction results and the variation curve of the fitness value are shown in Figs. 4 and 5, respectively.

The prediction results of the test set were translated into current imbalance codes according to Table 1, and the prediction accuracies of the test set for the three sets of station data reached 95.1, 97.8, and 97.2%. These high-accuracy predictions indicate that the prediction method closely approximates the actual variation of current imbalance rate. This prediction model is based on the current sensor module of the smart meter to collect data for the three-phase current to achieve the early warning of the current unbalance condition of the transformer, enabling the implementation of a series of compensation methods, such as current compensation by switching a power regulator,[18] model control based on combined switching states,[19] distributed selective harmonic mitigation, and decoupling unbalance compensation by coordinated inverters,[20] as mentioned in the literature. These compensation methods can be applied in a timely and targeted manner to control current balance, thereby reducing line losses and mitigating the risk of faults.

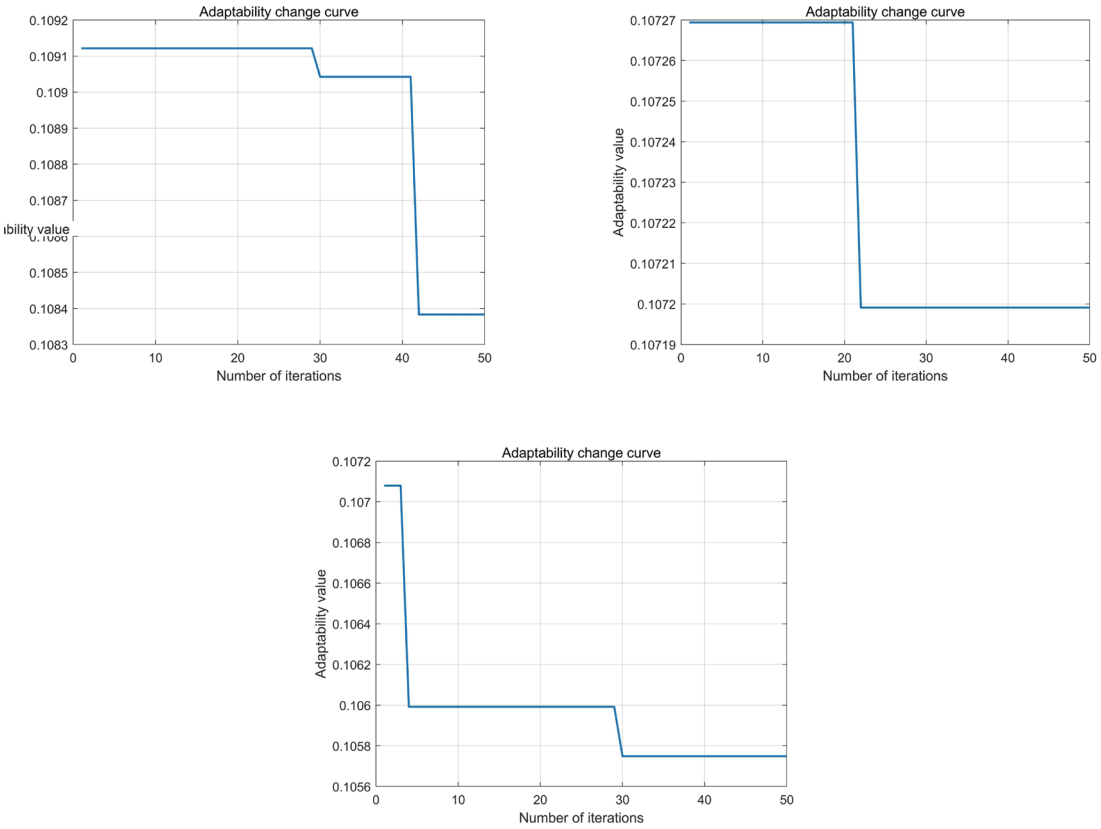

Fig. 4. (Color online) Network training adaptation curve for three station areas.

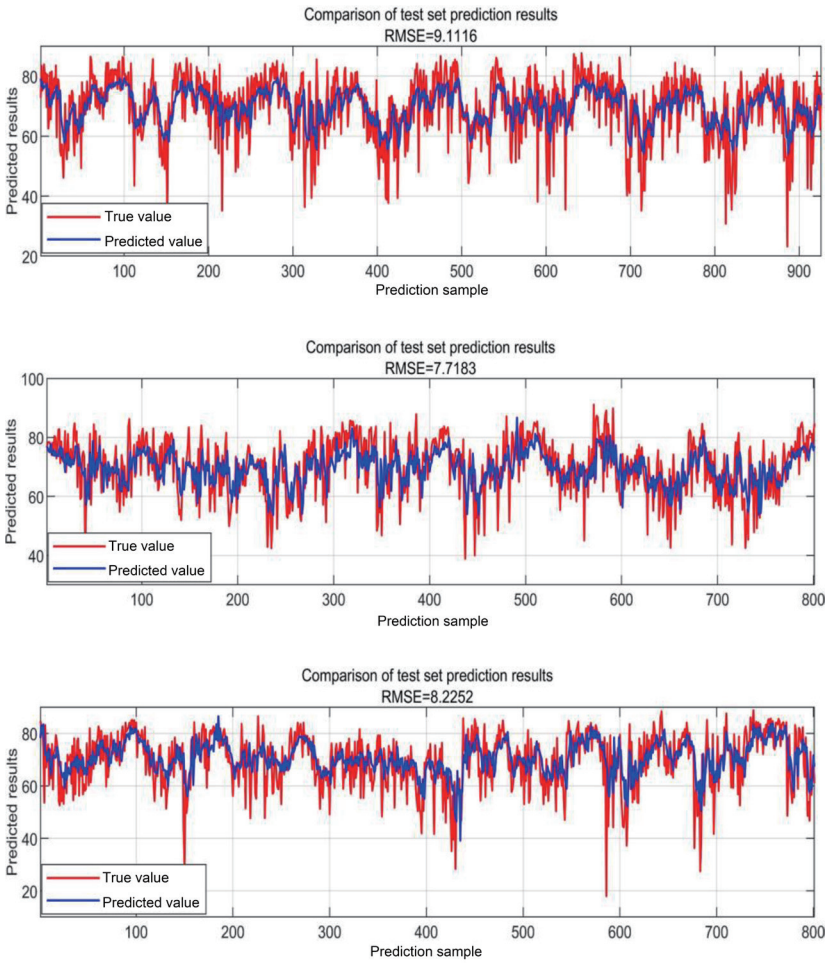

Fig. 5. (Color online) Prediction results for the test set for three station areas.

3.4 Comparison of prediction errors with other network models

To further evaluate the performance of the GA-optimized neural network model in predicting transformer current balance rate timing, additional comparison experiments were conducted using the BP and RBF neural network timing prediction model on the same dataset. These model were trained and tested on the current balance timing data, and their prediction errors were compared with those of the GA-optimized model.

The RBF network utilizes radial basis functions as hidden units to create a high-dimensional space in the hidden layer. This transformation of the input vector allows for the linear separability of the data in the higher space, making it capable of handling nonlinear functions and capturing complex patterns within the system. The RBF network exhibits excellent generalization capability and fast learning convergence, making it suitable for nonlinear function approximation tasks. Table 2 shows the average error test and the prediction accuracy results for each of the three models for 10 training sessions.

Table 2
Training result error test table.

Algorithm	Station area number	R^2	*RMSE*	Code prediction accuracy (%)
GA-BP	1	0.32826	9.3917	96.5
	2	0.28959	7.8944	97.2
	3	0.36916	8.1352	96.9
BP	1	0.21969	10.0731	94.3
	2	0.23734	8.9882	95.3
	3	0.31201	8.7362	94.9
RBF	1	0.25139	9.8737	95.1
	2	0.23166	8.6672	95.4
	3	0.32245	8.5650	95.2

After conducting multiple training sessions, the findings reveal that the GA-BP neural network outperforms both the pure BP network and the RBF network in terms of prediction accuracy and adaptability. Despite the longer training process associated with the GA-BP algorithm, its prediction results are characterized by higher confidence and greater stability.

4. Conclusions

In this paper, a current balance timing prediction model based on the GA-BP neural network is proposed, which utilizes the population search of the GA to optimize the neuron weights and thresholds in the process of training the BP neural network, resulting in improved prediction accuracy. The model is applied to the real-world data collected from a smart meter metering system, which provides transformer current data for calculating the current imbalance degree and classifying the imbalance state through coding. After preprocessing, the current imbalance rate time series data is obtained, and several tests are conducted to determine the optimal neural network structure and GA parameters for the model. The performance of the optimized GA-BP model is compared with that of a pure BP model using practical transformer current timing data from three typical low-voltage residential customer stations. The results demonstrate that the optimized model yields better prediction results with lower errors, indicating its considerable feasibility in balance state prediction. However, note that the presence of missing values in real-time metering data from smart meters may impact the prediction accuracy, potentially resulting in reduced prediction effectiveness for the balance state due to the missing values. Despite this limitation, the framework of the three-phase current balance state prediction proposed in this study can serve as a practical reference for fault prediction and line loss measurement in power systems. The use of a grid-based smart meter metering system, combined with balance compensation technology, has the potential to reduce transformer losses and fault incidence by accurately predicting the three-phase balance state.

Acknowledgments

This work was supported by the science and technology project of Yunnan Power Grid Co., Ltd., which provided funding under project number YNKJXM20220010.

References

1 S. Tao, J. Shen, Y. Song, and S. Guan: Int. J. Electr. Power Energy Syst. **150** (2023) 109076. https://doi.org/10.1016/j.ijepes.2023.109076
2 Z. Xing, Y. He, J. Chen, X. Wang, and B. Du: Electr. Power Syst. Res. **215** (2023) 109016. https://doi.org/10.1016/j.epsr.2022.109016
3 L. Chang: Power Syst. Technol. **12** (2001) 52. https://doi.org/10.13335/j.1000-3673.pst.2001.12.013
4 H. Fang, W. Sheng, J. Wang, Y. Liang, J. Wang, and S. Wang: Power Syst. Technol. **9** (2015) 2185. https://doi.org/10.13334/j.0258-8013.pcsee.2015.09.011
5 Z. Qu: China Venture Capital **9** (2017) 144. https://doi.org/10.3969/j.issn.1673-5811.2017.09.135
6 J. Pan, J. Liu, X. Chen, and K. Zhou: Energy Reports. **7** (2021) 312. http://gfbfh81f8000da3924570so0qkbbf6ovof6boq.fgac.kust.cwkeji.cn/10.1016/j.egyr.2021.01.064
7 L. Zheng: Ind. Mine Autom. **8** (2021) 90. https://doi.org/10.13272/j.issn.1671-251x.17694
8 X. Cui, Z. Ma, Z. Zhong, and C. Weng: Mod. Electr. Power **6** (2013) 38. https://doi.org/10.3969/j.issn.1007-2322.2013.06.008
9 G. Weng, Y. Gong, J. Shu, and F. Huang: Chinese High Technol. Lett. **7** (2020) 687. https://doi.org/10.3772/j.issn.1002-0470.2020.07.004
10 A. Pasdar and H. H. Mehne: Int. J. Electr. Power Energy Syst. **33** (2011) 693. https://doi.org/10.1016/j.ijepes.2010.11.019
11 W. Yang, X. Kang, X. Wang, and M. Wang: Energy Reports **9** (2023) 1830. https://doi.org/10.1016/j.egyr.2022.12.079
12 F. Zhao, S. Li, X. Chen, Y. Wang, F. Zhang, X. Niu, and Y. Gan: Power Syst. Technol. **3** (2022) 870. https://doi.org/10.13335/j.1000-3673.pst.2021.0413
13 X. Zeng, H. Zhai, M. Wang, M. Yang, and M. Wang: Int. J. Electr. Power Energy Syst. **113** (2021) 618. https://doi.org/10.1016/j.ijepes.2019.05.038
14 Y. Manabe and B. Chakraborty: Neurocomput. **70** (2007) 1360. https://doi.org/10.1016/j.neucom.2006.06.005
15 A. Sboev, A. Serenko, R. Rybka, D. Vlasov, and A. Filchenkov: Proc. Comput. Sci. **145** (2018) 488. https://doi.org/10.1016/j.procs.2018.11.111
16 S.Mou, X.Qi, and Q.Liu: Smart Power **12** (2010) 55. https://doi.org/10.3969/j.issn.1673-7598.2010.12.015
17 S. Tongchim and P. Chongstitvatana: Inf. Process. Lett. **82** (2002) 47. https://doi.org/10.1016/S0020-0190(01)00286-1
18 M. D. B. Gomes, M. C. Cavalcanti, L. R. Limongi, G. Azevedo, and M. Brito: Int. J. Electr. Power Energy Syst. **138** (2021) 107881. https://doi.org/10.1016/j.ijepes.2021.107881
19 H. Li, C. Pan, X. Ge, L. Guo, and Y Li: Int. J. Electr. Power Energy Syst. **125** (2021) 106554. https://doi.org/10.1016/j.ijepes.2020.106554
20 A. M. d. S. Alonso, D. I. Brandao, E. Tedeschi, and F. P. Marafao: Electr. Power Syst. Res. **186** (2020) 106407. https://doi.org/10.1016/j.epsr.2020.106407

About the Authors

Yiming Zhang was born in 1990 in Chuxiong, Yunnan Province. He graduated from Kunming University of Science and Technology in 2014 and is now an engineer at the Metering Center (Power Load Control Technology Center) of Yunnan Power Grid Co. His main research directions are grid digitization, power metering automation, and network security for power monitoring systems. (zhangyiming01@im.yn.csg)

Xiaohua Yang was born in 1988 in Jingdong County, Yunnan Province. He graduated from Yunnan University in 2011 with a major in electronic information and is currently an engineer and senior technician at the Metering Center (Power Load Control Technology Center) of Yunnan Power Grid Co. His main research directions are smart electricity usage and marketing metering. (yangxiaohua01@im.yn.csg)

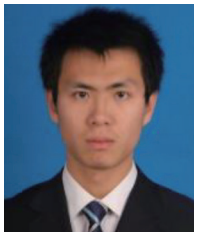

Tingjie Ba was born in 1985 in Gongyi City, Henan Province. He graduated from Kunming University of Technology in 2016 with a degree in electrical engineering and is currently the senior manager of the Marketing Department of Yunnan Power Grid Co. His main research directions are the demand-side response of meters, new energy access, the optimization of vehicle–pile network power interaction, the economic operation of virtual power plants, and the precise load management of new power systems.
(batingjie@im.yn.csg)

Yuang Lin was born in 2002 in Chaozhou City, Guangdong Province. Currently, he is a sophomore in the School of Information Engineering and Automation at Kunming University of Science and Technology and is pursuing a bachelor's degree in data science and big data technology with major research interests in artificial intelligence, data analytics, and data mining. (18087147030@163.com)

Yonghui Zhao was born in 1987 in Qujing City, Yunnan Province. He graduated from North China Electric Power University in 2013, majoring in control, and is now the manager of the Metering Center of Yunnan Power Grid Co. His main research direction is electrical energy metering.
(676808913@qq.com)